

## Rat Mesenchymal Stromal Cell Sheets Suppress Renal Fibrosis via Microvascular Protection

AYA IMAFUKU <sup>a</sup>, MASATOSHI OKA,<sup>b,c</sup> YOEI MIYABE,<sup>b</sup> SACHIKO SEKIYA,<sup>a</sup> KOSAKU NITTA,<sup>b</sup> TATSUYA SHIMIZU<sup>a</sup>

**Key Words.** Fibrosis • Kidney • Microvessels • Mesenchymal stem cell • Tissue engineering • Stem cell transplantation • Cytokines

<sup>a</sup>Institute of Advanced Biomedical Engineering and Science, Tokyo Women's Medical University, Tokyo, Japan; <sup>b</sup>Department of Nephrology, Tokyo Women's Medical University, Tokyo, Japan; <sup>c</sup>Cell Sheet Tissue Engineering Center (CSTEC), Department of Pharmaceutics and Pharmaceutical Chemistry, Health Sciences, University of Utah, Salt Lake City, Utah, USA

Correspondence: Tatsuya Shimizu, M.D., Ph.D., Institute of Advanced Biomedical Engineering and Science, Tokyo Women's Medical University, 8-1 Kawada-cho, Shinjuku-ku, Tokyo 162-8666, Japan. Telephone: 81-3-3353-8112; e-mail: shimizu.tatsuya@twmu.ac.jp

Received April 10, 2019; accepted for publication September 4, 2019; first published November 1, 2019.

<http://dx.doi.org/10.1002/sctm.19-0113>

This is an open access article under the terms of the Creative Commons Attribution-NonCommercial-NoDerivs License, which permits use and distribution in any medium, provided the original work is properly cited, the use is non-commercial and no modifications or adaptations are made.

### ABSTRACT

Renal fibrosis is one of the largest global health care problems, and microvascular (MV) injury is important in the development of progressive fibrosis. Although conventional cell therapy suppresses kidney injury via the role of vasoprotective cytokines, the effects are limited due to low retention of administered cells. We recently described that transplantation of hepatocyte growth factor (HGF)-transgenic mesothelial cell sheets showed a remarkable cell survival and strong therapeutic effects in a rat renal fibrosis model. Due to the translational hurdles of transgenic cells, we here applied this technique for allogeneic transplantation using rat bone marrow mesenchymal stromal cells (MSCs). MSC sheets were transplanted onto the kidney surface of a rat renal ischemia–reperfusion-injury model and the effects were compared between those in untreated rats and those receiving intravenous (IV) administration of the cells. We found that donor-cell survival was superior in the cell sheet group relative to the IV group, and that the cell sheets secreted HGF and vascular endothelial growth factor (VEGF) up to day 14. Transplantation of cell sheets increased the expression of activated HGF/VEGF receptors in the kidney. There was no evidence of migration of transplanted cells into the kidney parenchyma. Additionally, the cell sheets significantly suppressed renal dysfunction, MV injury, and fibrosis as compared with that observed in the untreated and IV groups. Furthermore, we demonstrated that the MSC sheet protected MV density in the whole kidney according to three-dimensional microcomputed tomography. In conclusion, MSC sheets strongly prevented renal fibrosis via MV protection, suggesting that this strategy represents a potential novel therapy for various kidney diseases. *STEM CELLS TRANSLATIONAL MEDICINE* 2019;8:1330–1341

### SIGNIFICANCE STATEMENT

Cell therapy has been applied to various diseases that are resistant to conventional therapy. Renal fibrosis is one of the most difficult issues, and many researchers have tried intravascular administration of stem cells. The present study revealed that transplantation of mesenchymal stromal cell (MSC) sheets onto the kidney showed dramatic effects, including long-term cell survival, amelioration of kidney dysfunction, vasoprotection, and antifibrosis, compared with intravenous administration of MSCs. These results suggest that cell sheet technology improves the effects of cell therapy in various aspects. Therefore, cell sheet therapy could be a potential novel therapeutic approach for various kidney diseases in the future.

### INTRODUCTION

Chronic kidney disease (CKD) is a worldwide problem associated with considerable morbidity and mortality, resulting in elevated health care costs [1, 2]. Regardless of its etiology, renal fibrosis is the final common pathway that correlates with the loss of renal function [3]. Currently, there remains no fundamental treatment for renal fibrosis.

Although acute kidney injury (AKI) was previously regarded as a reversible condition, recent studies suggest a strong link between AKI and

subsequent development of CKD [4–7]. Furthermore, growing evidence supports the important contribution of renal microvascular (MV) injury to the initiation and subsequent extension of kidney injury [4, 8, 9]. In contrast with renal tubular cells, endothelial cells exhibit little regenerative capacity [4, 10, 11], and irreversible MV loss following endothelial injury induces renal hypoxia and accelerates tubulointerstitial injury [10–13]. Moreover, MV loss is common in any form of CKD, regardless of etiology, and strongly correlates with fibrosis progression [14, 15]. Recently, Ehling et al. reported the evidence of MV loss in

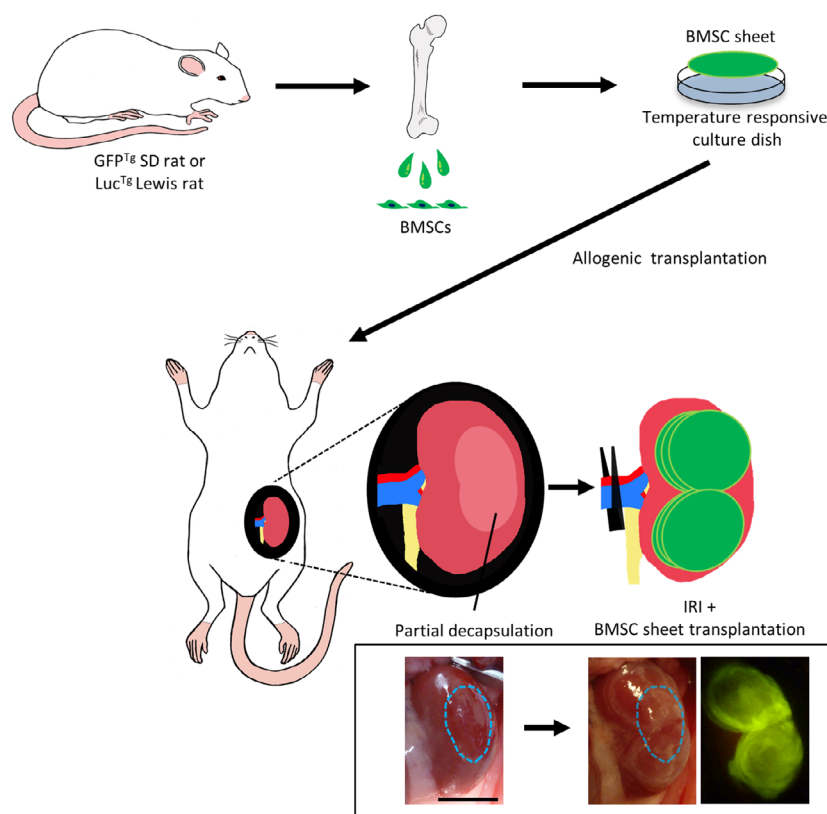


**Figure 1.** Schematic diagram illustrating the procedure for transplantation of bone marrow mesenchymal stromal cell (BMSC) sheets onto the kidneys of a rat ischemia–reperfusion-injury (IRI) model. Rat BMSCs were isolated from green fluorescent protein transgenic (GFP<sup>Tg</sup>) Sprague-Dawley rats or luciferase transgenic (Luc<sup>Tg</sup>) Lewis rats, and BMSC sheets were created using temperature-responsive culture dishes. After removing part of the abdominal renal capsule, six cell sheets (two sets of three-layered cell sheets) were placed on the abdominal side including the exposed area. Treatment effects were compared among Sham, IRI, and intravenous groups. Scale bar: 1,000 mm.

the whole kidney using *ex vivo* microcomputed tomography ( $\mu$ CT) [15]. Although administration of vasoprotective and antifibrotic cytokines, including hepatocyte growth factor (HGF) and vascular endothelial growth factor (VEGF), for kidney diseases have been attempted [16–19], they did not achieve adequate effects due to their short half-life [20, 21]. Furthermore, many researchers have tried systemic administration of cells secreting these cytokines [22–27], but the effects were limited because of low survival of transplanted cells into the kidney. We recently applied “cell sheet technology,” which enables direct transplantation and long-term survival of the cells to treat kidney disease [28]. Transplantation of human mesothelial cell (MC) sheets transfected with a vector expressing *HGF* (an HGF-tg MC sheet) on the kidney surface of a rat renal fibrosis model resulted in long-term survival of transplanted cells and strong therapeutic effects in the whole kidney. In this previous study, after removing part of the renal capsule, which is mainly composed of MCs, MC sheets were orthotopically transplanted onto the exposed area; the transplanted MCs survived for a long time and showed renoprotective effects via HGF secreted from MCs.

Therefore, we invented a method to apply this cell sheet therapy for various kidney diseases. If long-term survival and renoprotective effects by cell sheet therapy could be achieved using cells other than MCs, that is, heterotopic transplantation, the application of cell sheet therapy for kidney diseases will expand. Here, we applied mesenchymal stromal cell (MSC)-sheet therapy for kidney disease. MSCs represent a feasible cell source for translational medicine, because they are easily isolated and

expanded from various tissues [29]. MSCs secrete various cytokines and repair injured organs through various mechanism, including vasoprotection, anti-inflammation, and immunomodulation [30]. Several studies reported the effect of MSC sheets under various conditions, including ischemic cardiac disease, diabetic foot ulcers, and osteonecrosis of the jaw [31–33]. Therapeutic effects were partially explained by cytokines secreted from MSCs, and additionally, it was also revealed that transplanted MSCs migrated into the target organs and differentiated into mural cells. To date, application of an MSC sheet for kidney disease has not been reported, and there is no knowledge about the behavior and therapeutic effects of the transplanted MSCs. In this study, we performed allogeneic transplantation of a rat bone marrow-derived MSC (BMSC) sheet onto the kidney surface of a rat renal ischemia–reperfusion-injury (IRI) model, which mimics renal vascular injury under the condition of kidney transplantation and aorta replacement therapy. We evaluated the behavior of the transplanted cells and antifibrotic effects associated with MV protection (Fig. 1).

## MATERIALS AND METHODS

### Ethics

All animal protocols were conducted in accordance with the Guide for the Care and Use of Laboratory Animals and were approved by the Animal Welfare Committee of Tokyo Women’s Medical University (animal experiments no. AE16-101, 17-116, 18-007, and 19-017).

### Isolation and Characterization of BMSC

Bone marrow cells were isolated from male Sprague-Dawley (SD) rats for *in vitro* experiments, as well as from SD<sup>Tg</sup> (CAG-enhanced green fluorescent protein [EGFP]) rats and Luc<sup>Tg</sup> Lewis rats [34], for *in vivo* experiments, as previously described [33]. Briefly, after cutting the epiphyses of femora and tibiae, the bone marrow cavity was flushed with complete medium (a-MEM; Minimum Essential Medium; Life Technologies, Carlsbad, CA, USA supplemented with 1% penicillin–streptomycin [Life Technologies, Rockville, MD, USA] and 10% fetal bovine serum [Japan BioSerum]), using a 23-gauge needle. The cell suspension was filtered using a 100- $\mu$ m cell strainer, centrifuged for 15 minutes at 700g at room temperature, and subsequently cultured in complete medium at 37°C in a 5% CO<sub>2</sub> incubator. One day after seeding, nonadherent cells were removed by washing with phosphate-buffered saline (PBS) and fresh medium was added. The medium was replaced every 2–3 days. The cells were passaged at 80%–90% confluence using 0.05% trypsin-ethylenediaminetetraacetic acid (Merck, Darmstadt, Germany) and expanded until passages 3–5. Cultured cells were evaluated for MSC characteristics according to the ability to differentiate into osteocytes and adipocytes, colony-forming ability, and cell-surface markers as previously described [33].

### Fabrication of BMSC Sheets

BMSCs derived from SD<sup>Tg</sup> (CAG-EGFP) rats at passages three through five were seeded onto 35-mm temperature-responsive culture dishes (CellSeed, Inc., Tokyo, Japan) at a density of  $1.2 \times 10^6$  cells per dish and cultured in 2 ml complete medium supplemented with 82  $\mu$ g/ml ascorbic acid. Following incubation for 2 days, BMSC sheets were detached from the dishes by reducing the temperature from 37°C to 20°C.

### Cytokine Secretion in BMSC-Culture Supernatant

The concentration of growth factors secreted into the BMSC-culture supernatant was measured by enzyme-linked immunosorbent assay (ELISA). BMSCs were seeded onto 35-mm culture dishes at a density of  $1.2 \times 10^6$  cells per dish. Since BMSC sheets were transplanted 2 days after seeding *in vivo* experiments, the time point at 2-days postseeding was defined as day 0. The medium was replaced with fresh complete medium on days 0, 5, 7, 12, and 14. VEGF and HGF levels on days 0, 7, and 14 were measured using ELISA kits (R&D Systems, Minneapolis, MN, USA;  $n = 5$  per group).

### IRI Procedure and BMSC Transplantation

SD rats (6-week-old males) were randomly divided into four groups: IRI ( $n = 15$ ), IRI + BMSC-sheet transplantation ( $n = 10$ ), IRI + IV administration of BMSCs ( $n = 10$ ), and Sham ( $n = 4$ ).

Under isoflurane anesthesia, rats were subjected to right nephrectomy. At 7 days after nephrectomy, IRI was performed by clamping left renal pedicle for 60 minutes. In BMSC-sheet group, BMSC sheets derived from SD<sup>Tg</sup> (CAG-EGFP) rats were transplanted onto the kidney. Approximately 1/3 of the abdominal capsule of the left kidney (1/6 of the whole capsule) was peeled off using tweezers, followed by transplantation of the BMSC sheets individually onto the kidney surface in order to cover the abdominal side of the kidney including the exposed area ( $n = 6$  sheets per rat), and IRI procedure was performed. For IV administration of BMSCs, we used  $7.2 \times 10^6$  cells, which was approximately equivalent to the number of cells in six sheets.

BMSCs were suspended in 1 ml of normal saline and administered via the tail vein soon following reperfusion. Sham-operated animals underwent right nephrectomy and laparotomy only without clamping of renal pedicle or any treatment. In the non-cell sheet-groups (Sham, IRI, and IV groups), the capsule was left intact.

For all rats, blood and urine samples were collected at the specific time points, and the animals were sacrificed at 14-days postsurgery. To evaluate the therapeutic effects during the initial phase, we performed additional animal experiments according to the same protocols except for right nephrectomy, with animals sacrificed on days 1, 4, and 7 ( $n = 1$ –4). At the indicated time points, left kidneys were excised and sections were prepared. For tissue homogenate analysis, after removing renal capsule, samples were snap-frozen in liquid nitrogen and stored at  $-80^\circ\text{C}$ .

### Bioluminescence Imaging

BMSCs derived from Luc<sup>Tg</sup> Lewis rats were transplanted as cell sheets or IV into SD rats ( $n = 4$  and  $n = 3$ , respectively). Bioluminescence imaging (BLI) was performed using a Xenogen IVIS 100 imaging system (PerkinElmer, Waltham, MA, USA) on days 0, 1, 4, 7, 10, and 14. D-Luciferin (Promega, Madison, WI, USA) was injected via the penile vein and the peak signal from a fixed region of interest was estimated.

### Kidney Function

Serum Cr and UN levels were analyzed on days 0, 1, 2, 4, 7, and 14 (Sham:  $n = 4$ ; IRI:  $n = 7$ ; IV:  $n = 6$ ; BMSC sheet:  $n = 9$ ).

### Histopathological Analysis

Paraffin-embedded sections were stained with periodic acid-Schiff (PAS), Masson-trichrome (MT) staining and immunolabeled with mouse anti- $\alpha$ -smooth muscle actin ( $\alpha$ SMA) antibody (M0851, Dako, Carpinteria, CA, USA), rat anti-endothelial cell antigen-1 (RECA-1) antibody (ab9774, Abcam, Cambridge, UK), and rabbit anti-phospho-cMet antibody (ab5662; Abcam), detected using peroxidase-conjugated polymer reagent (EnVision, K4061; Dako). Phospho-cMet staining was performed by Pathology Institute Corp. (Toyama, Japan). Cryosections were stained with mouse anti-GFP antibody (A11120, Thermo Fisher Scientific, Waltham, MA, USA), goat anti-kidney injury molecule-1 (KIM-1) antibody (AF3689, R&D Systems), mouse anti-CD54 (intercellular adhesion molecule-1 [ICAM-1]) antibody (554,967, BD Pharmingen, San Diego, CA, USA), rabbit anti-laminin antibody (ab11575, Abcam), rabbit anti-fibronectin antibody (ab23751, Abcam), and rabbit anti-phospho-VEGF receptor (VEGFR)-1 antibody (AF6204, Affinity Biosciences, San Jose, CA, USA). For quantification, five micrographs of the cortex from each rat were acquired randomly. The degree of tubular injury was assessed based on established methods [35, 36]. In brief, we graded the extent of tubular necrosis, urinary casts, brush border loss, and tubular dilatation as follows: 0:<10%; 0.5:10-25%; 1:25-45%, 1.5:45-75%, and 2:>75%. The fractional areas harboring  $\alpha$ SMA, fibrosis, RECA-1 luminal area, phospho-cMet, and phospho-VEGFR-1 were analyzed using ImageJ software (National Institutes of Health). For quantification of MV density, the ratio of microvessels to tubules and RECA-1-stained fraction area in the cortex was calculated according to a method described previously [14, 15].

### Urinary Analysis

To evaluate tubular injury, urinary KIM-1 on day 4 was measured using an ELISA kit (R&D Systems; IRI:  $n = 5$ ; Sham, IV, and BMSC sheet:  $n = 4$ ).

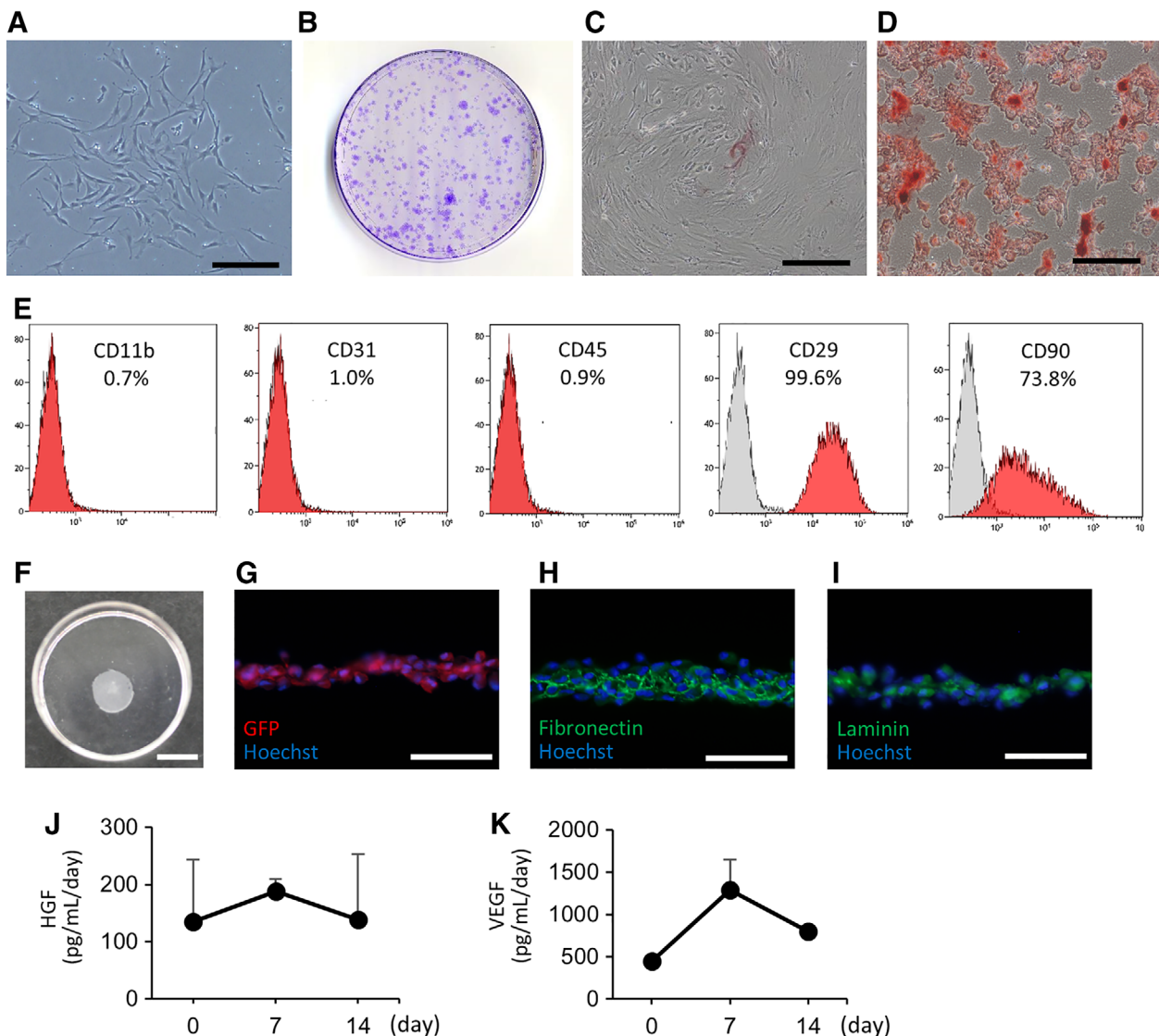


**Figure 2.** Characteristics of bone marrow mesenchymal stromal cells (BMSCs) and BMSC sheets. **(A):** Cultured bone marrow cells displayed a spindle-shaped appearance. Scale bar: 100  $\mu\text{m}$ . **(B):** Colony forming assay showing multiple colonies stained with crystal violet. **(C):** Cells cultured in osteoinductive medium showing alizarin red S-positive calcium deposits. Scale bar: 200  $\mu\text{m}$ . **(D):** Cells cultured in adipogenic medium showing Oil Red O-positive lipid droplets. Scale bar: 200  $\mu\text{m}$ . **(E):** Flow cytometric analysis showing that cultured cells were positive for CD29 and CD90 and negative for CD11b, CD31, and CD45. **(F):** The appearance of a BMSC sheet fabricated using a temperature-responsive culture dish. Scale bar: 1,000 mm. **(G–I):** Immunohistology of BMSC sheets shows positivity for green fluorescent protein, fibronectin, and laminin. Scale bar: 50  $\mu\text{m}$ . **(J, K):** Rat BMSC sheets secreted hepatocyte growth factor and vascular endothelial growth factor up to day 14 *in vitro*.

### Total Collagen in the Kidney

The total collagen concentration within whole kidney (Sham:  $n = 4$ ; IRI, IV, and BMSC sheet:  $n = 5$ ) was determined using total collagen assay kit (Quickzyme, Leiden, The Netherlands).

### Levels of HGF and VEGF in the Kidney Tissue and Urine

Snap-frozen kidney tissues were minced into 1–2 mm pieces and homogenized using tissue homogenizer (CG-4A, BRT) in PBS. An equal volume of Cell Lysis Buffer 2 (895347, R&D Systems) was added and tissues were lysed at room temperature for 30 minutes and centrifuged at 20,000g at 4°C. The levels of HGF and VEGF in the tissue homogenate samples on day 4 (IRI, IV, BMSC sheet:  $n = 3$ ) and urinary samples on day

7 (BMSC sheet:  $n = 5$ ; IRI, IV:  $n = 4$ ) were measured using an ELISA kit (R&D Systems).

### Three-Dimensional Evaluation of Renal Microvasculature

Microfil (Flow Tech, Carver, MA, USA), a silicone rubber contrast agent, was perfused on a separate group of rats as previously described [15, 37, 38]. SD rats were randomly divided into three groups (IRI, IRI + BMSC sheet, and Sham [ $n = 5$  per group]). At 14-days postsurgery, a catheter was inserted into the aorta distal to the renal arteries and Microfil (at a MV112:MV diluent: curing agent ratio of 2.5:225 ml) was perfused at a rate of 3–4 ml/min per 100 g body weight. After fixing kidneys in 4% PFA, the kidneys were scanned by high-resolution  $\mu\text{CT}$  (R\_mCT2; Rigaku, Tokyo, Japan) and analyzed using Osirix software (Pixmeo, Bernex,

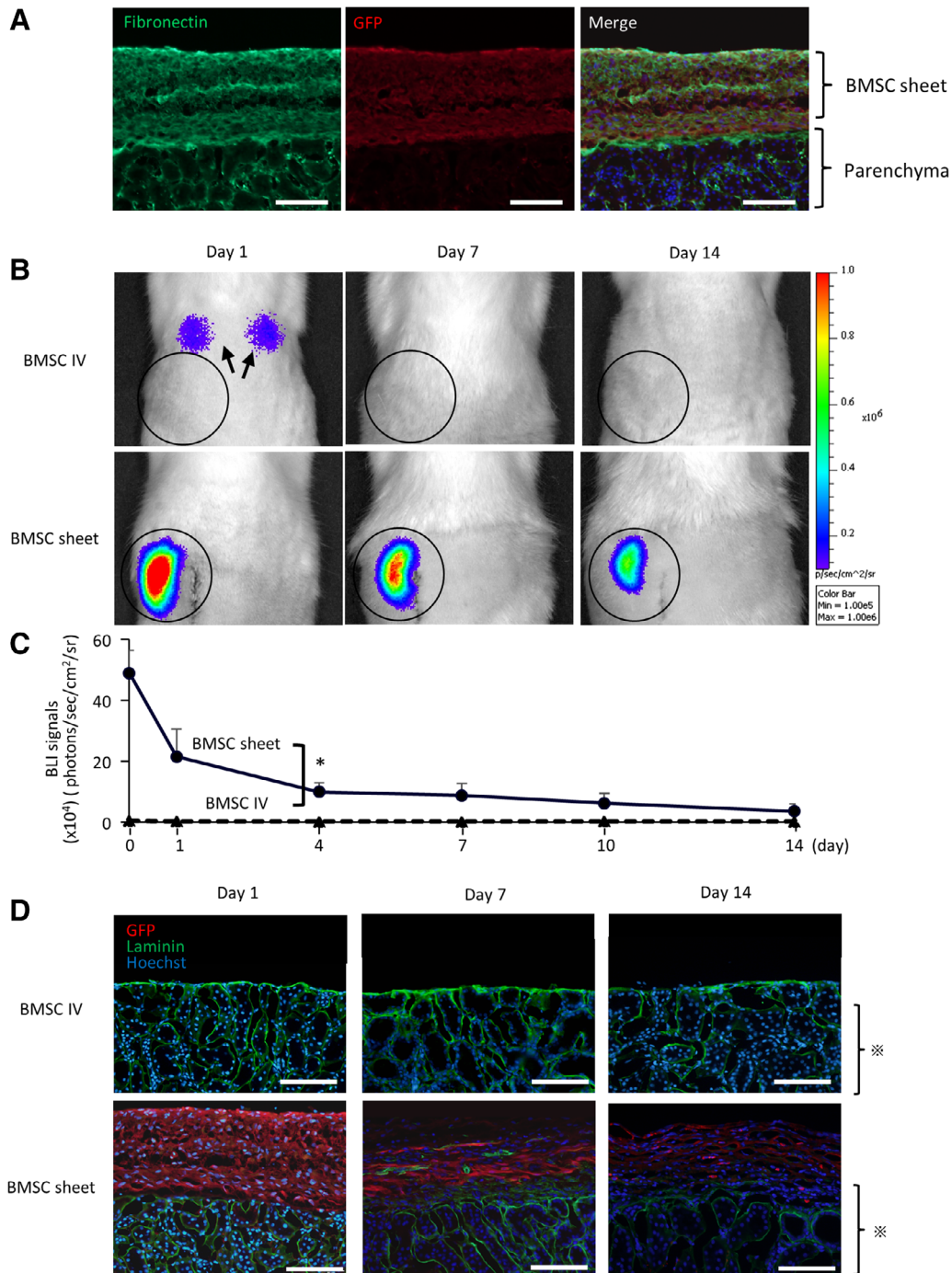


**Figure 3.** Retention of bone marrow mesenchymal stromal cells (BMSCs) after transplantation. **(A):** BMSC sheets contained fibronectin and attached on the kidney surface accordingly. Scale bar: 100  $\mu$ m. **(B, C):** Bioluminescence imaging following BMSC-sheet transplantation (black line) revealing superior retention of donor cells as compared with those injected (black dotted line). In the intravenous (IV) group, pulmonary embolism was observed (arrow). **(D):** In the BMSC-sheet group, green fluorescent protein-expressing BMSCs (shown in red color) were observed on the kidney surface until day 14, with no accompanying migration of the transplanted cells into the parenchyma (\*). Green is laminin and blue is Hoechst. Scale bar: 200  $\mu$ m; \*,  $p < .05$ .

Switzerland). According to threshold-based blood-vessel segmentation, the ratio of small-vessel volume per kidney volume was calculated in order to analyze MV density in the whole kidney. Then kidneys were bisected longitudinally and dehydrated in alcohol and methyl salicylate, and visualization was performed using a stereomicroscope.

### Statistical Analysis

Data were expressed as mean  $\pm$  SEM. Differences were analyzed using Student's  $t$  test or analysis of variance (ANOVA), followed by Tukey's post hoc comparison test and time-dependent data were analyzed by one-way repeated-measures ANOVA, using JMP Pro14 software. A  $p < .05$  was considered significant.

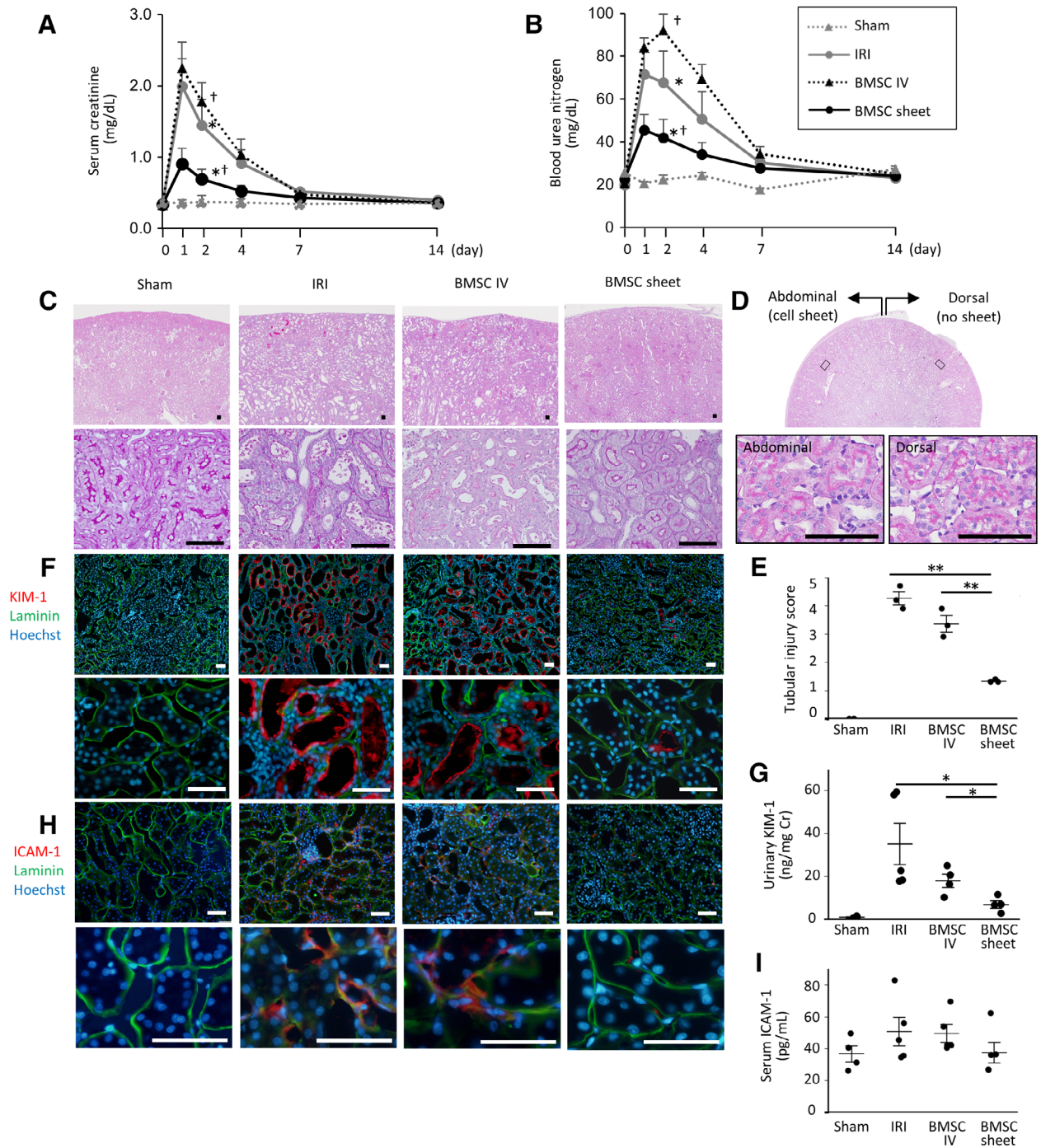


**Figure 4.** Assessment of kidney function, tubular, and endothelial injury following bone marrow mesenchymal stromal cell (BMSC)-sheet transplantation. **(A, B):** In the BMSC-sheet group (black lines), elevations in serum creatine and blood urea nitrogen levels were significantly lower than those in the ischemia–reperfusion-injury (IRI; gray lines) and intravenous (IV; black dotted lines) groups (\*,  $p < .05$ , IRI vs. BMSC sheet; †,  $p < .05$ , BMSC sheet vs. BMSC IV). **(C):** Periodic acid-Schiff staining showing severe tubular necrosis in the ischemia–reperfusion-injury (IRI; black arrow) group, whereas the tubular epithelium is well preserved in the BMSC-sheet group on day 4. Scale bar: 100  $\mu$ m. **(D):** Transverse section of kidney in the BMSC sheet group shows that there was no difference in the histology between abdominal side (with cell sheets) and dorsal side (without cell sheets). **(E):** Tubular injury score was significantly lower in the BMSC sheet group compared with the IRI and IV groups. **(F):** The kidney injury molecule-1 (KIM-1)-positive proximal tubule area (shown in red color) in the BMSC-sheet group was smaller than that of the IRI group. Green is laminin and blue is Hoechst. Scale bar: 100  $\mu$ m. **(G):** Urinary KIM-1 levels were significantly lower in the BMSC-sheet group than those in the IRI and IV groups. **(H):** The intercellular adhesion molecule-1 (ICAM-1)-positive endothelial cell area (shown in red color) in the BMSC-sheet group was smaller than that of the IRI group. Green is laminin and blue is nuclear staining (Hoechst). Scale bar: 100  $\mu$ m. **(I):** Serum ICAM-1 levels tended to be lower in the BMSC-sheet group than those in the IRI and IV groups; \*,  $p < .05$ ; \*\*,  $p < .01$ .

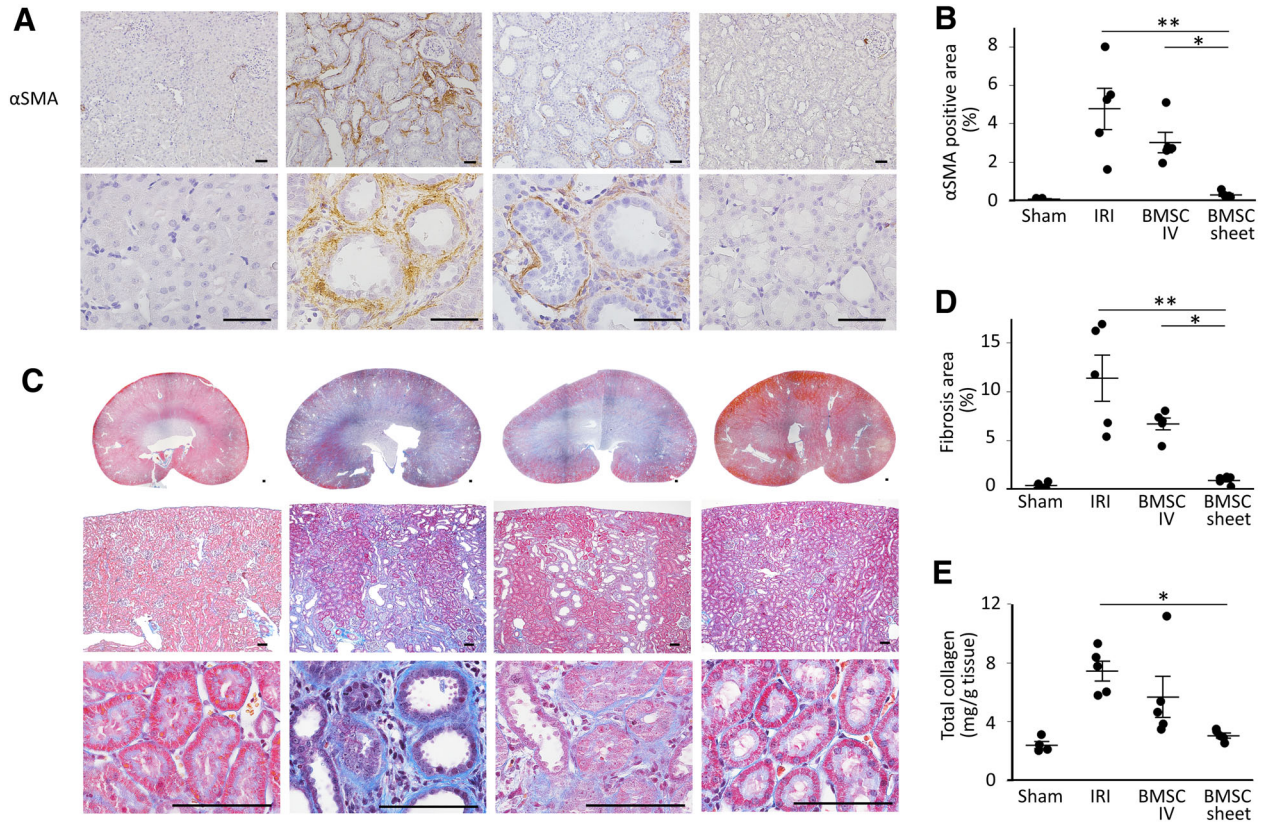


**Figure 5.** Assessment of renal fibrosis following bone marrow mesenchymal stromal cell (BMSC)-sheet transplantation. **(A, B)**: The number of  $\alpha$ -smooth muscle actin ( $\alpha$ SMA)-positive myofibroblasts was significantly lower in the BMSC-sheet group relative to that observed in the ischemia–reperfusion-injury (IRI) and intravenous (IV) groups. Scale bar: 50  $\mu$ m. **(C, D)**: Masson-trichrome staining showing significant reductions in the fibrotic area in the BMSC-sheet group as compared with that observed in the IRI and IV groups. Scale bar: 100  $\mu$ m. **(E)**: Total collagen in the whole kidney was significantly lower in the BMSC-sheet group relative to that observed in the IRI group; \*,  $p < .05$ ; \*\*,  $p < .01$ .

## RESULTS

### BMSC Phenotype

Cultured cells showed a typical spindle-shaped appearance (Fig. 2A), self-renewal ability (Fig. 2B), and the ability to differentiate into osteocytes and adipocytes (Fig. 2C, 2D). Flow cytometric analysis revealed positivity for CD29 and CD90 and negativity for CD11b, CD31, and CD45 (Fig. 2E). These findings confirmed the presence of an MSC phenotype.

### BMSC Sheets Secreted Vasoprotective Cytokines *in vitro* until Day 14

After detachment, the BMSC sheets shrunk to  $0.97 \pm 0.11$  cm in diameter (Fig. 2F). To evaluate the levels of cytokines secreted from the BMSC sheets, we measured cytokine concentrations in the culture supernatant. Figure 2J, 2K shows HGF and VEGF concentrations in the supernatant of cultured BMSCs, with levels at day 14 of  $276 \pm 228$  pg/ml per day and  $1,597 \pm 117$  pg/ml per day, respectively. Thus, we observed secretion of HGF and VEGF *in vitro* until day14.

### BMSC Sheets Remained on the Kidney Surface for up to 14 Days

BMSC sheets contained laminin and fibronectin (Fig. 2H, 2I) and readily attached to the kidney surface *in vivo* on day 1 (Fig. 3A). We assessed *in vivo* retention of transplanted BMSCs from Luc<sup>T8</sup>

rats by BLI (Fig. 3B, 3C). Although the intensity of the BLI signal decreased during the observation period, the signal in the BMSC-sheet group confirmed the presence of surviving cells in the left renal area up to day 14. By contrast, in the group that received cells intravenously (intravenous [IV] group), the signal was undetectable in the left renal areas at all time points, although signals were detected in the lungs, suggesting the presence of pulmonary embolism. For GFP immunostaining (Fig. 3D), GFP-expressing BMSCs were not detected at any time point in the IV group, whereas in the BMSC-sheet group, GFP-expressing BMSCs were observed around the kidney capsule up to day 14 but without migration into the parenchyma. These results confirmed that the BMSC sheets remained on the kidney surface for up to 14 days.

### BMSC Sheets Ameliorated Renal Dysfunction

Kidney function at different time points is shown in Figure 4A, 4B. In the BMSC-sheet group, elevations in Cr and UN levels were significantly lower than those observed in the IRI and IV groups. BMSC-sheet transplantation ameliorated renal dysfunction.

### BMSC Sheets Ameliorated Tubular and Endothelial Injury

In order to evaluate tubular injury, PAS staining and immunostaining for KIM-1, a proximal tubular injury marker, and ELISA for urinary KIM-1 were performed using kidney specimen and urine on day 4. The tubular injury was significantly milder in the BMSC-sheet group compared with the IRI and IV group (Fig. 4C, 4E,

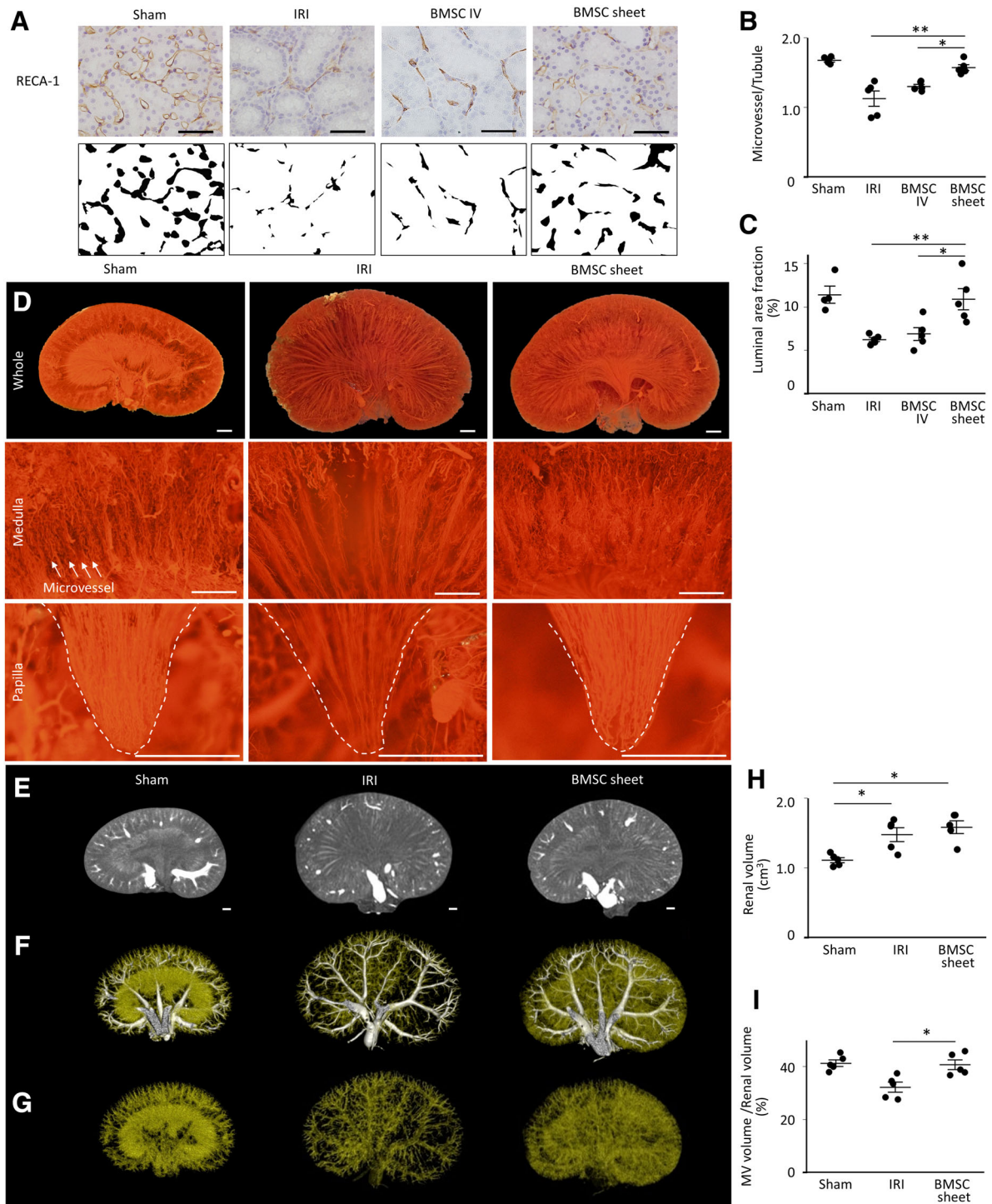


**Figure 6.** The effect of bone marrow mesenchymal stromal cell (BMSC)-sheet transplantation on microvascular (MV) injury. **(A):** Representative images of rat endothelial cell antibody (RECA)-1-positive microvasculature (upper) and RECA-1-stained fraction areas transformed into binary images (lower) in the cortex. Scale bar: 50  $\mu\text{m}$ . **(B):** MV density (the ratio of microvessels to tubules) was significantly higher in the BMSC-sheet group as compared with that in the ischemia–reperfusion-injury (IRI) and intravenous (IV) groups. **(C):** RECA-1-stained fraction area was significantly higher in the BMSC-sheet group as compared with that in the IRI and IV groups. **(D):** Representative Microfil patterns observed by low-power stereomicroscopy. In the BMSC-sheet group, MV density was well preserved as compared with that in the IRI group (upper, whole kidney; middle, medulla; and lower, papilla). Scale bar: 1,000  $\mu\text{m}$ . **(E, H):** According to three-dimensional microcomputed tomography analysis, kidney volume in the ischemia–reperfusion-injury (IRI) and BMSC-sheet groups significantly increased relative to that in the Sham group. **(F–I):** The small-vessel volume per kidney volume in the BMSC-sheet group increased significantly relative to that observed in the IRI group (white, large vessel; yellow, small-vessel). Scale bar: 1,000  $\mu\text{m}$ ; \*\*,  $p < .01$ ; \*,  $p < .05$ .

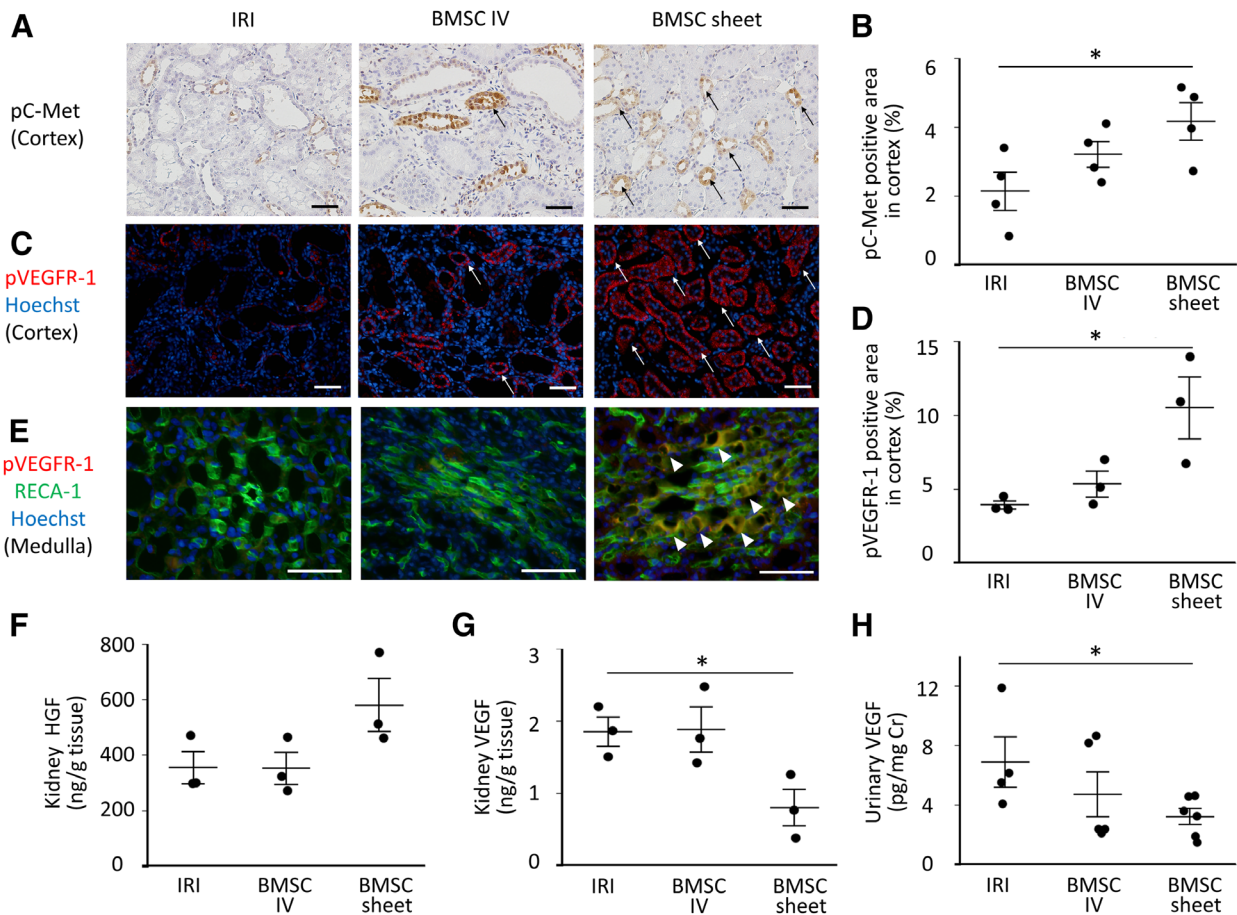


**Figure 7.** Assessment of hepatocyte growth factor (HGF)/vascular endothelial growth factor (VEGF) and their activated receptors in the kidneys following bone marrow mesenchymal stromal cell (BMSC)-sheet transplantation. **(A, B):** The area of phospho-C-met-positive tubules (black arrow) was significantly higher in the BMSC-sheet group relative to that observed in the ischemia–reperfusion-injury (IRI) group. Scale bar: 50  $\mu$ m. **(C, D):** The area of phospho-VEGFR-1-positive tubules (white arrow) was significantly higher in the BMSC-sheet group relative to that observed in the IRI group. Scale bar: 50  $\mu$ m. **(E):** In the BMSC-sheet group, phospho-VEGFR-1-positive endothelial cells (white arrowhead) was observed in the medulla; \*,  $p < .05$ . **(F):** The level of HGF in kidney tissue tended to be higher in the cell sheet group compared to the IRI group. **(G, H):** The level of VEGF in kidney tissue and urine was significantly lower in the cell sheet group compared to the IRI group.

Supporting Information Fig. S3). Additionally, KIM-1-positive area in the BMSC-sheet group was smaller than that in the IRI and IV groups (Fig. 4F), with urinary KIM-1 levels significantly lower in the BMSC-sheet group relative to those in the IRI and IV groups (Fig. 4G). In the BMSC-sheet group, the treatment effect was homogenous throughout the kidney, even in locations not covered by cell sheets (Fig. 4D). Furthermore, in order to evaluate endothelial injury, immunostaining for ICAM-1 was performed using kidney samples on day 4 and serum ICAM-1 was measured using serum samples on day 1. The ICAM-1 positive endothelial cell areas in the BMSC-sheet group were smaller than those in the IRI and IV groups (Fig. 4H), and serum ICAM-1 levels tended to be lower in the BMSC-sheet group relative to those in the IRI and IV groups (Fig. 4I). These results indicate that BMSC-sheet ameliorated tubular injury and endothelial injury.

### BMSC Sheets Suppressed Renal Fibrosis

In the BMSC-sheet group,  $\alpha$ -SMA-positive areas were significantly fewer relative to those in the IRI and IV groups on day 14 (Fig. 5A, 5B). Similarly, MT staining demonstrated significant reductions in the fibrotic area in the BMSC-sheet group as compared with that in the IRI and IV groups (Fig. 5C, 5D). As shown in the whole kidney

section staining, the antifibrotic effect was homogenous in the entire kidney. Furthermore, the BMSC-sheet group displayed a significantly lower amount of total collagen in the whole kidney relative to that in the IRI group ( $7.5 \pm 0.7$  mg/g tissue vs.  $3.1 \pm 0.2$  mg/g tissue;  $p < .05$ ; Fig. 5E). These data indicated that BMSC-sheet transplantation suppressed fibrosis.

### BMSC Sheets Preserved MV Density in the Entire Kidney

Since it is known that MV-density loss caused by endothelial injury results in progressive fibrosis, MV density was evaluated using kidney specimen on day 14 (Fig. 6A–6C). In the BMSC-sheet group, the ratio of microvessels to tubules was significantly higher than that observed in the IRI and IV groups ( $1.6 \pm 0.04$  vs.  $1.1 \pm 0.1$  and  $1.3 \pm 0.1$ ;  $p < .05$ ). Additionally, the area of the RECA-1-stained fraction was significantly larger in the BMSC-sheet group as compared with that in the IRI and IV groups ( $10.9\% \pm 1.2\%$  vs.  $6.3\% \pm 0.2\%$  and  $6.9\% \pm 0.4\%$ ;  $p < .05$ ). In order to determine MV density in the whole kidney, Microfil perfusion into the renal microvasculature were performed. Figure 6D shows representative filling patterns under stereomicroscopy in the Sham, IRI, and BMSC-sheet groups. IRI resulted in considerable reductions in MV

density in the whole kidney, especially in the renal medulla and papilla, which are vulnerable to ischemia. On the other hand, MV density was well preserved in the BMSC-sheet group. We then performed 3D-volume rendering of reconstructed  $\mu$ CT data (Fig. 6E–6G), finding significantly increased kidney volumes in both the IRI and BMSC-sheet groups due to kidney injury, relative to that in the Sham group (Fig. 6E, 6H). According to a threshold-based method, vessels were segmented by large vessels (Fig. 6F; white) and small vessels (Fig. 6F, 6G; yellow), with the small-vessel volume per kidney volume in the BMSC-sheet group significantly larger than that in the IRI group ( $40.6\% \pm 1.8\%$  vs.  $32.2\% \pm 1.9\%$ ;  $p < .05$ ; Fig. 6I). These results indicated that BMSC-sheet transplantation preserved MV density in the entire kidney.

### BMSC Sheets Increased the Expression of Activated HGF/VEGF Receptors in the Kidney

Immunostaining of phospho-C-Met showed a significant increase of activated HGF-receptors in the cortical tubules in the BMSC sheet group relative to those in the IRI groups on day 14 (Fig. 7A, 7B). Similarly, the expression of phospho-VEGF-R1 positive tubules in the cortex was significantly higher than those in the IRI groups on day 4 (Fig. 7C, 7D). Furthermore, while we could identify phospho-VEGF-R1-positive endothelial cells in the medulla of the BMSC sheet group, no positive endothelial cells were found in the IRI group (Fig. 7E). Taken together, these data suggest that the transplantation of cell sheets activated HGF and VEGF receptors in the kidney. Additionally, we measured concentration of HGF/VEGF in homogenate kidney tissue and urine. As a result, we showed that the concentration of HGF in kidney tissue tended to be higher in BMSC sheet group compared with the IRI group, suggesting a supply of HGF to the kidney from the cell sheet (Fig. 7F). On the hand, the level of VEGF in kidney tissue and urine was significantly lower in cell sheet group compared with the IRI group (Fig. 7G, 7H).

## DISCUSSION

In this study, we tested the hypothesis that transplantation of a BMSC-sheet would suppress renal fibrosis in a renal IRI model via long-term protection of the microvasculature. Our results indicate that BMSC sheet attached on the kidney surface, possibly by the retained ECM in the BMSC sheet, and remained on the kidney surface for 14 days, and that the survival of donor cells was superior in the BMSC-sheet group as compared with that in the IV group. There was no evidence of migration into the renal parenchyma nor embolism of transplanted cells. As a consequence of the superior survival of the transplanted cells on the kidney surface in the BMSC-sheet group, we observed superior suppression of renal dysfunction, tubular injury, endothelial injury, loss of MV density, and fibrosis relative to those in the IRI and IV groups, indicating that the BMSC sheet suppressed transition into progressive fibrosis via long-term vasoprotection. BMSC sheets secreted HGF and VEGF up to day 14, suggesting the ability of the sheets to continuously secrete these cytokines following *in vivo* transplantation. Furthermore, the expression of activated HGF/VEGF receptors was higher in the BMSC sheet group relative to those in the IRI group, which could be an effect of the transplanted cell sheets. Therefore, MV protection was likely, at least partially, due to the effect of HGF and VEGF secretion from the cell sheets. Supporting Information Figure S4

shows the schematic diagram of the therapeutic mechanism of the BMSC-sheet described in the present study.

The BMSC sheet attached and remained on the kidney surface and resulted in the strong suppression of kidney injury. As we show in this study, cell sheets preserve the adhesive ECM such as fibronectin and laminin underlying their bottom surfaces, because it does not require enzymatic digestion [39, 40]. Therefore, cell sheets can adhere to the target organ directly and sustain long-term survival. For example, hepatocyte sheets transplanted into the subcutaneous space survive for >200 days while maintaining the biological functions [41]. Since the therapeutic effect of cell therapy is thought to be derived from factors secreted from transplanted cells [22–27, 42], it is generally believed that prolonged presence of donor cells in the target organs leads to improved efficacy. Indeed, the long-term survival of the cell sheets on the target organ resulted in stronger therapeutic effects as compared with injection of cells in various disease models [31–33]. Furthermore, we previously showed that transplantation of an HGF-tg MC-sheet onto the kidney surface suppressed kidney injury to a significantly greater degree than remote transplantation (on femoral vascular bed) of the HGF-tg MC-sheets [28]. Accordingly, in the present study, the long-term survival of transplanted cells on the kidney surface resulted in strong therapeutic effects.

Transplantation of BMSC sheets suppressed endothelial injury, loss of MV density and transition into progressive kidney fibrosis. Protection of MV density by the BMSC sheets might have resulted in suppression of tubulointerstitial injury caused by hypoxia. Previous reports showed that restoration of MV density or renal blood flow improved oxygenation of the kidney [12, 43]. Therapeutic approaches targeting chronic hypoxia, including protection of microvasculature, have been reported to suppress fibrosis [12, 13, 16–18]. Therefore, our results suggested that the BMSC sheet suppressed tubular injury and transition into progressive fibrosis via protection of renal microvasculature.

Here, the vasoprotective cytokines secreted from the BMSC sheet might have contributed to renal MV protection. In our study, there was no evidence of migration of the transplanted cells into the kidney parenchyma; this indicates that there was no differentiation of transplanted cells in the kidney, suggesting that the therapeutic effects resulted from the effect of cytokines secreted from BMSCs. These results are consistent with those for transplantation of HGF-tg MC sheets for kidney disease, which suggested that the therapeutic effect was derived by the role of HGF [28]. Transplantation of BMSC sheets increased the level of HGF in the kidney, activated HGF receptors in tubules and suppressed renal fibrosis. It has been reported that high level of HGF in the kidney contributes to suppression of kidney injury and fibrosis [44]. Furthermore, transplantation of BMSC sheets activated VEGF receptors in tubule and endothelial cells and ameliorated MV injury. The level of VEGF in the kidney tissue and urine was lower in the BMSC sheet group, a finding, which initially might seem contradictory considering that the BMSC sheets secrete VEGF. However, it is known that the level of VEGF in kidney and urine increases after kidney injury as VEGF is induced by hypoxia [45, 46]. Therefore, low level of VEGF in the kidney tissue and urine in the BMSC sheet group might be explained by suppression of hypoxia. These results suggested that therapeutic effect was partially achieved by vasoprotective cytokines secreted from BMSC sheets.

BMSC sheet transplantation was superior to intravascular administration of BMSCs in terms of safety. In our study, the

number of injected cells was 3–7 times higher than previous reports [22–24]. Therefore, in contrast to other studies, IV administration of BMSCs did not show any effects in terms of kidney function based on serum Cr and blood urea nitrogen. Since paracrine effects of MSCs depend on the number of cells [47], therapeutic effects are expected to be stronger when the number of transplanted cells increase. However, at the same time, mortality increases due to pulmonary embolism. For example, Furlani et al. reported that 40% of mice died due to pulmonary embolism when  $1 \times 10^6$  cells ( $=40 \times 10^6/\text{kg}$ , when body weight is 25 g) were injected in bloodstream [48]. In our study, the dose of MSCs was approximately  $30 \times 10^6/\text{kg}$ , and animals in IV group showed pulmonary embolism. As a result, the animals' general conditions were bad in the initial phase, they did not gain sufficient weight and mortality rate was 30% (Supporting Information Figs. S1 and S2), consistent with previous reports which administered similar amount of MSCs. On the other hand, despite the many studies using cell sheets, none has reported embolism, even when a large number of cells were transplanted. Therefore, we believe that cell sheet technology is a promising form of cell therapy, which can obtain strong therapeutic effect using many cells without unfavorable effects.

This is the first study demonstrating the efficacious use of transplanted BMSC sheets to treat kidney disease. Transplantation of BMSC sheets protected microvasculature in the whole kidney and strongly suppressed fibrosis via the effects of vasoprotective cytokines secreted from BMSC sheets, in the absence of unfavorable adverse effects. The biggest advantage of this study is that we applied cells other than MCs for cell therapy to treat kidney disease. To date, various kinds of cytokines and cell therapies have been reported to be effective for kidney diseases. Our results suggest the possibility to expand the application of cell sheet therapy for various kidney diseases using many kinds of cells and cytokines. Furthermore, BMSC sheet transplantation could be applied under conditions of kidney transplantation and aortic replacement therapy to prevent transition into progressive kidney disease caused by IRI. This is feasible because it requires no additional invasion for cell sheet transplantation. Moreover, since MV loss leads to fibrosis in CKD regardless of etiology, there is a possibility that transplantation of BMSC sheets can suppress progressive fibrosis in various kidney diseases. Therefore, cell sheet therapy could be a potential novel therapeutic approach for various kidney diseases in the future.

Our study has some limitations. Although we focused on the role of HGF and VEGF, we did not evaluate associated cell-signaling pathways based on Western blotting, or the effects of *HGF* and *VEGF* knockdown in the context of BMSC effectiveness. Moreover, because the mechanism associated with the therapeutic effects of MSCs appears multifaceted, we cannot exclude the possibility of the influence of other factors. Therefore, an exhaustive analysis of the roles of various cytokines is required to clarify the exact mechanism associated with the therapeutic efficacy of the BMSC sheet.

## CONCLUSION

Our results demonstrated that BMSC-sheet transplantation for a rat renal IRI model suppressed renal fibrosis via MV protection.

## ACKNOWLEDGMENTS

We thank Hidekazu Sekine and Nobuyuki Kaibuchi for technical support. This work was supported by JSPS KAKENHI grant number 15K21386. This work was also supported by a fund from CellSeed, Inc.

## AUTHOR CONTRIBUTIONS

A.I., M.O.: conception and design, collection and assembly of data, data analysis and interpretation, manuscript writing; Y.M., S.S., N.K., T.S.: data analysis and interpretation, final approval of manuscript.

## DISCLOSURE OF POTENTIAL CONFLICTS OF INTEREST

Tatsuya Shimizu is a member of the scientific advisory board, a shareholder and received research funding from CellSeed, Inc. The other authors indicated no potential conflicts of interest.

## DATA AVAILABILITY STATEMENT

The data that support the findings of this study are available from the corresponding author, upon reasonable request.

## REFERENCES

- Hoerger TJ, Simpson SA, Yarnoff BO et al. The future burden of CKD in the United States: A simulation model for the CDC CKD Initiative. *Am J Kidney Dis* 2015;65:403–411.
- Honeycutt AA, Segel JE, Zhuo X et al. Medical costs of CKD in the medicare population. *J Am Soc Nephrol* 2013;24:1478–1483.
- Nath KA. Tubulointerstitial changes as a major determinant in the progression of renal damage. *Am J Kidney Dis* 1993;20:1–17.
- Basile DP, Donohoe D, Roethe K et al. Renal ischemic injury results in permanent damage to peritubular capillaries and influences long-term function. *Am J Physiol Renal Physiol* 2001;281:F887–F899.
- Bucaloiu ID, Kirchner HL, Norfolk ER et al. Increased risk of death and de novo chronic kidney disease following reversible acute kidney injury. *Kidney Int* 2012;81:477–485.
- Coca SG, Singanamala S, Parikh CR. Chronic kidney disease after acute kidney injury: A systematic review and meta-analysis. *Kidney Int* 2012;81:442–448.
- Forbes JM, Hewitson TD, Becker GJ et al. Ischemic acute renal failure: Long-term histology of cell and matrix changes in the rat. *Kidney Int* 2000;57:2375–2385.
- Sutton TA, Mang HE, Campos SB et al. Injury of the renal microvascular endothelium alters barrier function after ischemia. *Am J Physiol Renal Physiol* 2003;285:F191–F198.
- Molitoris BA, Sutton TA. Endothelial injury and dysfunction: Role in the extension phase of acute renal failure. *Kidney Int* 2004;66:496–499.
- Basile DP, Friedrich JL, Spahic J et al. Impaired endothelial proliferation and mesenchymal transition contribute to vascular rarefaction following acute kidney injury. *Am J Physiol Renal Physiol* 2011;300:F721–F733.
- Basile DP, Zeng P, Friedrich JL et al. Low proliferative potential and impaired angiogenesis of cultured rat kidney endothelial cells. *Microcirculation* 2012;19:598–609.
- Nangaku M. Chronic hypoxia and tubulointerstitial injury: A final common pathway to end-stage renal failure. *J Am Soc Nephrol* 2006;17:17–25.

- 13** Tanaka S, Tanaka T, Nangaku M. Hypoxia as a key player in the AKI-to-CKD transition. *Am J Physiol Renal Physiol* 2014;307:F1187–F1195.
- 14** Babickova J, Klinkhammer BM, Buhl EM et al. Regardless of etiology, progressive renal disease causes ultrastructural and functional alterations of peritubular capillaries. *Kidney Int* 2017;91:70–85.
- 15** Ehling J, Babickova J, Gremse F et al. Quantitative micro-computed tomography imaging of vascular dysfunction in progressive kidney diseases. *J Am Soc Nephrol* 2016;27:520–532.
- 16** Kang DH, Hughes J, Mazzali M et al. Impaired angiogenesis in the remnant kidney model: II. Vascular endothelial growth factor administration reduces renal fibrosis and stabilizes renal function. *J Am Soc Nephrol* 2001;12:1448–1457.
- 17** Iliescu R, Fernandez SR, Kelsen S et al. Role of renal microcirculation in experimental renovascular disease. *Nephrol Dial Transplant* 2010;25:1079–1087.
- 18** Leonard EC, Friedrich JL, Basile DP. VEGF-121 preserves renal microvessel structure and ameliorates secondary renal disease following acute kidney injury. *Am J Physiol Renal Physiol* 2008;295:F1648–F1657.
- 19** Gong R, Rifai A, Dworkin LD. Anti-inflammatory effect of hepatocyte growth factor in chronic kidney disease: Targeting the inflamed vascular endothelium. *J Am Soc Nephrol* 2006;17:2464–2473.
- 20** Ido A, Moriuchi A, Kim I et al. Pharmacokinetic study of recombinant human hepatocyte growth factor administered in a bolus intravenously or via portal vein. *Hepatol Res* 2004;30:175–181.
- 21** Takeshita S, Zheng LP, Brogi E et al. Therapeutic angiogenesis. A single intraarterial bolus of vascular endothelial growth factor augments revascularization in a rabbit ischemic hind limb model. *J Clin Invest* 1994;93:662–670.
- 22** Togel F, Hu Z, Weiss K et al. Administered mesenchymal stem cells protect against ischemic acute renal failure through differentiation-independent mechanisms. *Am J Physiol Renal Physiol* 2004;289:F31–F42.
- 23** Togel F, Weiss K, Yang Y et al. Vasculotropic, paracrine actions of infused mesenchymal stem cells are important to the recovery from acute kidney injury. *Am J Physiol Renal Physiol* 2007;292:F1626–F1635.
- 24** Togel F, Zhang P, Hu Z et al. VEGF is a mediator of the renoprotective effects of multipotent marrow stromal cells in acute kidney injury. *J Cell Mol Med* 2009;13:2109–2114.
- 25** Duffield JS, Bonventre JV. Kidney tubular epithelium is restored without replacement with bone marrow-derived cells during repair after ischemic injury. *Kidney Int* 2005;68:1956–1961.
- 26** Yuan L, Wu MJ, Sun HY et al. VEGF-modified human embryonic mesenchymal stem cell implantation enhances protection against cisplatin-induced acute kidney injury. *Am J Physiol Renal Physiol* 2011;300:F207–F218.
- 27** B L, Cohen A, Hudson TE et al. Mobilized human hematopoietic stem/progenitor cells promote kidney repair after ischemia/reperfusion injury. *Circulation* 2010;121:2211–2220.
- 28** Oka M, Sekiya S, Sakiyama R et al. Hepatocyte growth factor-secreting mesothelial cell sheets suppress progressive fibrosis in a rat model of chronic kidney disease. *J Am Soc Nephrol* 2019;30:261–276.
- 29** Caplan AI. Mesenchymal stem cells. *J Orthop Res* 2011;9:641–650.
- 30** Caplan AI, Correa D. The MSC: An injury drugstore. *Cell Stem Cell* 2011;9:11–15.
- 31** Narita T, Shintani Y, Ikebe C et al. The use of scaffold-free cell sheet technique to refine mesenchymal stromal cell-based therapy for heart failure. *Mol Ther* 2013;21:860–867.
- 32** Kato Y, Iwata T, Morikawa S et al. Allogeneic transplantation of an adipose-derived stem cell sheet combined with artificial skin accelerates wound healing in a rat wound model of type 2 diabetes and obesity. *Diabetes* 2015;64:2723–2734.
- 33** Kaibuchi N, Iwata T, Yamato M et al. Multipotent mesenchymal stromal cell sheet therapy for bisphosphonate-related osteonecrosis of the jaw in a rat model. *Acta Biomater* 2016;42:400–410.
- 34** Hakamata Y, Murakami T, Kobayashi E. “Firefly rats” as an organ/cellular source for long-term in vivo bioluminescent imaging. *Transplantation* 2006;81:1179–1184.
- 35** Solez K, Morel-Maroger L, Sraer JD. The morphology of “acute tubular necrosis” in man: Analysis of 57 renal biopsies and a comparison with the glycerol model. *Medicine* 1979;58:362–376.
- 36** Kelleher SP, Robinette JB, Miller F et al. Effect of hemorrhagic reduction in blood pressure on recovery from acute renal failure. *Kidney Int* 1987;31:725–730.
- 37** Iliescu R, Chade AR. Progressive renal vascular proliferation and injury in obese Zucker rats. *Microcirculation* 2010;17:250–258.
- 38** Ortiz MC, Garcia-Sanz A, Bentley MD et al. Microcomputed tomography of kidneys following chronic bile duct ligation. *Kidney Int* 2000;58:1632–1640.
- 39** Okano T, Yamada N, Okuhara M et al. Mechanism of cell detachment from temperature-modulated, hydrophilic–hydrophobic polymer surfaces. *Biomaterials* 2006;16:297–303.
- 40** Kushida A, Yamato M, Konno C et al. Decrease in culture temperature releases monolayer endothelial cell sheets together with deposited fibronectin matrix from temperature-responsive culture surfaces. *J Biomed Mater Res* 1999;45:355–362.
- 41** Ohashi K, Yokoyama T, Yamato M et al. Engineering functional two- and three-dimensional liver systems in vivo using hepatic tissue sheets. *Nat Med* 2007;13:880–885.
- 42** Sjoqvist S, Ishikawa T, Shimura D et al. Exosomes derived from clinical-grade oral mucosal epithelial cell sheets promote wound healing. *J Extracell Vesicles* 2019;8:1565264.
- 43** Saad A, Dietz AB, Herrmann SMS et al. Autologous mesenchymal stem cells increase cortical perfusion in renovascular disease. *J Am Soc Nephrol* 2017;28:2777–2785.
- 44** Morigi M, Rota C, Montemurro T et al. Life-sparing effect of human cord blood-mesenchymal stem cells in experimental acute kidney injury. *STEM CELLS* 2010;28:513–522.
- 45** Vaidya VS, Waikar SS, Ferguson MA et al. Urinary biomarkers for sensitive and specific detection of acute kidney injury in humans. *Clin Transl Sci* 2008;1:200–208.
- 46** Villanueva S, Céspedes C, Vio CP. Ischemic acute renal failure induces the expression of a wide range of nephrogenic proteins. *Am J Physiol Regul Integr Comp Physiol* 2006;290:R861–R870.
- 47** Sukho P, Kirpensteijn J, Hesselink JW et al. Effect of cell seeding density and inflammatory cytokines on adipose tissue-derived stem cells: An in vitro study. *Stem Cell Rev* 2017;13:267–277.
- 48** Furlani D, Ugurlucan M, Ong L et al. Is the intravascular administration of mesenchymal stem cells safe? Mesenchymal stem cells and intravital microscopy. *Microvasc Res* 2009;77:370–376.



See [www.StemCellsTM.com](http://www.StemCellsTM.com) for supporting information available online.